MIT Libraries | DSpace@MIT

MIT Open Access Articles

Distributed Control of an Ill-Conditioned Non-Linear Process Using Control Relevant Excitation Signals

Massachusetts Institute of Technology

Article

Distributed Control of an Ill-Conditioned Non-Linear Process Using Control Relevant Excitation Signals

Yusuf Abubakar Sha'aban

Department of Electrical Engineering, University of Hafr Al Batin, Hafar Al Batin 31991, Saudi Arabia; shaaban@uhb.edu.sa

Abstract: Efficient control schemes for ill-conditioned systems, such as the high-purity distillation column, can be challenging and costly to design and implement. In this paper, we propose a distributed control scheme that utilizes well-designed excitation signals to identify the system. Unlike traditional systems, we found that a summation of correlated and uncorrelated signals can yield better excitation of the plant. Our proposed distributed model predictive control (MPC) scheme uses a shifted input sequence to address loop interactions and reduce the computational load. This approach deviates from traditional schemes that use iteration, which can increase complexity and computational load. We initially tested the proposed method on the linear model of a highly coupled 2×2 process and compared its performance with decentralized proportional-integral-derivative (PID) controllers and centralized MPC. Our results show improved performance over PID controllers and similar results to centralized MPC. Furthermore, we compared the performance of the proposed approach with a centralized MPC on a nonlinear model of a distillation column. The results for the second study also demonstrated comparable performance between the two controllers with the decentralised control slightly outperforming the centralised MPC in some cases. These findings are promising and may be of interest to practitioners that are more comfortable with tuning decentralised loops.

Keywords: distributed control; ill-conditioned process; control-relevant excitation; model predictive control; distributed model predictive control; decoupling

1. Introduction

Ill conditioned non-linear processes are standard in the process industries. Such systems are characterized by high loop interaction and directionality, making them challenging to model and control. A typical example of such a process is the high-purity distillation column. The first step in most control design methods is to obtain a suitable model. The ability of the obtained model to capture the plant dynamics impacts the quality of control that can be achieved. Moreover, depleting resources means that the use of the available resources needs to be optimized. This requirement for the optimal usage of resources and the need to reduce product variability make the development of accurate models imperative. Therefore, the availability of such models will lead to an improvement in process control.

The challenges associated with identifying and controlling ill-conditioned systems mean that unusual steps are necessary for the development of plant excitation signals, the identification process and controller design [1–3]. Typical systems require that the excitation signals used for identification be uncorrelated for the proper excitation of the plant to obtain informative data for identification. However, for ill-conditioned systems, intelligent utilization of partially correlated plant excitation inputs has been demonstrated to generate informative data, yielding better results [4–7]. The work in [5] presents practical steps for the effective identification of industrial processes. In [8], the performance of an open-loop signal was compared with closed-loop generated signals for subspace identification. The models obtained from the closed-loop tests gave better performance both in terms of error in the frequency response and when used for model predictive control design.

The work presented in [9] developed a method for the identification of ill-conditioned systems using output rotation. To identify models in output directions that are control-relevant, the least-squares technique was employed to generate autoregression with exogenous input (ARX) models. However, prior to the development of such models, the outputs were rotated using principal component analysis (PCA). In [10], three methods for designing excitation signals to avoid correlated outputs in highly coupled systems were developed. These methods were based on the full state space model, an approximate covariance model and a simple dynamic gain matrix. When compared based on their speeds of execution, the methods displayed varying performances depending on the system under study. However, these techniques have not found wide adoption by industrial control practitioners.

The primary aim of any identification exercise is to obtain a control-relevant model. Hence, any benefits resulting from such an exercise need to be consolidated by an excellent controller. PID control has remained the most adopted controller in industrial and other applications [11]. This popularity has been linked to historical reasons: the availability of off-the-shelf hardware and ease of implementation. Its parameters i.e., the proportional, integral and derivative gains contribute control actions that are proportional to the current, historic and future errors, respectively. Hence, these parameters collaborate to eliminate these error components.

Therefore, PID is the default controller to be considered by most practitioners. However, standard PID controllers cannot address the interaction and coupling associated with ill-conditioned systems. Therefore, a range of decentralized PID (DPID) controllers have been proposed in the literature. Some of the most adopted DPID by industries were proposed in [12,13]. Both controllers have been successful in the industry and have motivated the development of several controllers [14,15]. The authors of [14] tuned a decentralized fractional order PID for two-input two-output (TITO) systems. In the work, a bat optimization algorithm was used to design diagonal fractional order PID controllers using a predetermined equivalent transfer function (ETF) model and decoupler. This was implemented on an interacting canonical tank-level process. An example of non standard implementation of PID is given in [16]. However, this work focuses on standard implementations which are easily implemented by most practitioners.

The recent drive towards the digitization and automation of industries towards the industry 4.0 paradigm shift means that there is the need to improve the performance of existing control loops. Moreover, about 30% of exisiting controllers are in manual mode while 41% of control loops are considered to have fair or poor performance [17].

Model predictive control (MPC) is the most influential advanced process control scheme for industrial applications. It has the inherent capability to handle process coupling and interactions naturally. Recently, MPC has found application in a variety of industries outside of process and manufacturing [18,19]. Despite this feat, the presence of MPC in the industry is still not as expected, considering its benefits and potential to revolutionize the industry. The complexity associated with managing extensive and interconnected systems has motivated the emergence of decentralized and distributed MPC (DMPC). Moreover, a significant number of existing industrial controlled systems are structured in a single-input, single-output (SISO) manner. Therefore, practitioners are quite comfortable with tuning SISO loops. Hence, considering the deployment of DMPC may appeal more to such practitioners, this may motivate a wider adoption of MPC to improve existing control loops performing poorly. Hence, studying these schemes on TITO systems is reasonable. Some studies in Distributed Model Predictive Control (DMPC) for extensive and interconnected processes are elucidated in these works [20–22]. Earlier works have also considered the relative performance of PID and MPC on dead-time dominant systems [23,24], while MPC was used to improve the performance of a PID with feedfoward in an industrial process in [25].

This paper proposes a decentralized MPC strategy to handle ill-conditioned TITO systems. However, the steps for obtaining informative data and a control-relevant model

are first explored to achieve these objectives. The developed scheme is compared with central MPC and decentralized PID controllers. The paper is therefore organized as follows. Section 2 is the methodology section. It discusses the details of the design of excitation signal, the different control algorithms used in the paper and details of the high-purity distillation column. The proposed DMPC approach is presented in Section 2.6. The outcomes are presented and critically analyzed within Section 3. The paper culminates with a conclusion in Section 4.

2. Methodology

2.1. The Skogestad and Morari Distillation Column

Distillation columns are among the most prevalent process systems in industrial applications. Therefore, over the past three to four decades, there has been research interest in the modelling and control of distillation columns. One of the most studied systems is the high-purity distillation column referred to as "Column A" [26–28]. In this paper, we only consider the input/output characteristics of the model. Details of the theory and assumptions used to develop the benchmark known as column A are given in [27]. The details of this are outside the scope of this work. The binary distillation column is a 4×4 system with inputs, outputs and measured disturbances as defined in Table 1.

Table 1. Process variables for the binary column.

Controlled Variables	Manipulated Variables	Measured Disturbances
Reflux flow (L)	Top composition (x_D)	Feed rate (F)
Boil-up flow (V)	Bottoms composition (x_B)	Feed composition (z_F)
Distillate flow (D)	Condenser boiler holdup (M_D)	Liquid fraction in feed (q_F)
Bottoms flow rate (B)	reboiler holdup (M_B)	-

The binary distillation can be configured in several ways based on input–output pairing. Some of these are the LV, DV and $(L/D)(V/B)$ configurations [26]. These configurations are achieved by closing some of the loops and using the remaining variables for control. In this paper, the LV-configuration, depicted in Figure 1, is adopted.
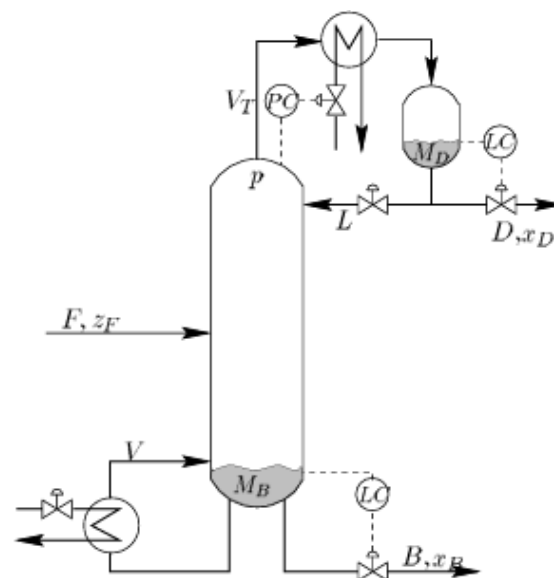
Figure 1. A simple Distillation Column Controlled with LV-Configuration [27].

In the LV-configuration, the loops for the distillate flow (D) and bottoms flow rate (B) are intially closed to ensure tight control. Then the reflux flow (L) is paired with the top

composition and boil-up flow (*V*) with bottoms composition. The resulting 2×2 system can therefore be represented (1).

$$\begin{bmatrix} x_D \\ x_B \end{bmatrix} = \begin{bmatrix} G_{11} & G_{12} \\ G_{21} & G_{22} \end{bmatrix} \begin{bmatrix} L \\ V \end{bmatrix} \tag{1}$$

The *LV*-configuration of this process is a non-linear system with directionally dependent dynamics. Therefore, it is imperative to take these factors into account when designing plant test signals and control strategy.

2.2. Manipulated-Variable Controlled-Variable (MV-CV) Pairing

Process interaction determines how the various manipulated variables (MVs) in a process affect the respective controlled variables (CVs). The most commonly adopted techniques for measuring the degree of process interaction are the singular value decomposition (SVD) and relative gain array (RGA) methods [29]. In this work, the RGA approach is adopted.

For a typical system represented by (2). Each of the outputs Y_1 and Y_2 are affected by both inputs U_1 and U_2.

$$Y(s) = G(s)U(s) \tag{2}$$

$$\begin{bmatrix} Y_1(s) \\ Y_2(s) \end{bmatrix} = \begin{bmatrix} G_{11} & G_{12} \\ G_{21} & G_{22} \end{bmatrix} \begin{bmatrix} U_1(s) \\ U_2(s) \end{bmatrix} \tag{3}$$

where

$$G_{11}(s) = \frac{K_{11}}{\tau_{11}s + 1} e^{-s\theta_{11}} \qquad G_{12}(s) = \frac{K_{12}}{\tau_{12}s + 1} e^{-s\theta_{12}}$$

$$G_{21}(s) = \frac{K_{21}}{\tau_{21}s + 1} e^{-s\theta_{21}} \qquad G_{22}(s) = \frac{K_{22}}{\tau_{22}s + 1} e^{-s\theta_{22}}$$

Let the matrix of process gains be defined as *K* and the matrix $H = (K^{-1})^T$. Then the RGA Λ is computed as follows [29]:

$$\Lambda = K \otimes H = \begin{bmatrix} \lambda_{ij} \end{bmatrix} \tag{4}$$

The operator $\otimes$ represents the Schur product such that $\lambda_{ij} = K_{ij}H_{ij}$.

$$K = \begin{bmatrix} K_{11} & K_{12} \\ K_{21} & K_{22} \end{bmatrix}; \quad \Lambda = \begin{bmatrix} \lambda & 1 - \lambda \\ 1 - \lambda & \lambda \end{bmatrix} \tag{5}$$

Note that for a TITO process, Λ is a symmetrical matrix: $\sum_i \lambda_{ij} = \sum_j \lambda_{ij} = 1$. Typically, $\lambda \leq 1$. A value of $\lambda \geq 0.5$ leads to the direct pairing of Y_1 with U_1, else reverse pairing is adopted [29].

2.3. Identification Test Signals

Identification tests are generally performed when plants are in operation. Hence, it is essential to develop plant friendly identification procedure that will have limited effect on the process. Since plant tests account for over three-quarters of the total costs associated with the deployment of advanced process controllers [30,31], it is imperative to determine optimized test signal magnitude and duration [5,32]. Several efficient excitation signals have been proposed in the literature. These include special noise signals such as the generalised binary noise (GBN) and filtered white noise. Other specially designed signals are the sum of sinusoids and pseudo random binary sequence (PRBS) [5,32,33]. PRBS signals ensure that the plant is not over excited outside its range of steady-state operations. Hence, the PRBS signal is adopted in this work. The details for designing appropriate PRBS signals are available in these works [30,32,33].

2.4. PID Decoupling Control

Numerous structures of the PID controller are available in the literature [11]. Moreover, several control companies and industries have their in-house structure and tuning methods. For its simplicity and prevalence, the ideal (or parallel) structure, described by (6), is adopted in this work.

$$k(s) = k_p + \frac{k_i}{s}s + k_d s \tag{6}$$

where the proportional, integral and derivative gains are represented by k_p, k_i and k_d respectively.

In highly coupled systems, multivariable controllers may be used to achieve defined control objectives. However, because of the difficulty associated with the tuning of multivariable PID controllers, decentralized controllers integrated with decouplers are often used. Usually, these decouplers are used to cancel the dynamics of non-paired loops. Several of these decouplers have been proposed over the years, some of which are presented in [34].

Assuming the utilization of a decoupling matrix D, the transformed transfer function $Q(s)$, following the decoupling process, is expressed as (7):

$$\begin{aligned} Q(s) &= G(s)D(s) \\ &= \begin{bmatrix} q_{11} & 0 \\ 0 & q_{22} \end{bmatrix} \end{aligned} \tag{7}$$

$$D(s) = \begin{bmatrix} 1 & d_{12}(s) \\ d_{21}(s) & 1 \end{bmatrix} \tag{8}$$

Hence, the parameters d_{12} and d_{21} can be computed using (9) as follows:

$$d_{12} = -\frac{G_{12}}{G_{11}} \qquad d_{21} = -\frac{G_{21}}{G_{22}} \tag{9}$$

Sometimes, the decoupler parameters d_{12} and d_{21} may not be physically implementable. For the sake of simplicity, *static decoupling* [35] is frequently employed. This method entails the utilization of a steady-state model, i.e., replacing the corresponding transfer functions with their steady-state gain values:

$$d_{12} = -\frac{K_{12}}{K_{11}} \qquad d_{21} = -\frac{K_{21}}{K_{22}} \tag{10}$$

Static decouplers have the drawback that interactions still occur in dissimilar loops during transients. However, the performance of such decouplers is sufficient for most loops during steady-state operations. The resulting decoupled process is subsequently controlled with a PID, which has the structure of (11). In situations where improved performance is required more sophisticated dynamic decouplers can be employed [36]. Owing to their wide acceptance by the research community and industry, two such items presented in [12,13] are adopted for comparison in this work.

$$K(s) = \begin{bmatrix} K_1 & 0 \\ 0 & K_2 \end{bmatrix} \tag{11}$$

The controllers $k_1(s)$ and $k_2(s)$ have the structure represented in (6) or any other PI/PID structure. Although, there is a recent trend in tuning PID controllers using optimization based methods, these methods have not shown better performance when compared to MPC controllers [23,24]. Moreover, these optimization based PID controllers have not found much application in industrial settings. Hence, we adopt PID controllers that have found industrial application [12,13].

2.4.1. PID with Lead-Lag Decoupling K_W

The PID controller proposed in [12] is tuned automatically and uses the lead-lag decoupler represented in (12).

$$D(s) = \begin{bmatrix} d_{11} & d_{12} \\ d_{21} & d_{22} \end{bmatrix} \tag{12}$$

The parameters d_{12} and d_{21} are defined in Equations (13) and (14).

$$d_{12} = -\frac{K_{12}}{K_{11}} \left(\frac{1 + \tau_{11}s}{1 + \tau_{12}s} \right) e^{-(\theta_{12} - \theta_{11})} \tag{13}$$

$$d_{21} = -\frac{K_{21}}{K_{22}} \left(\frac{1 + \tau_{22}s}{1 + \tau_{21}s} \right) e^{-(\theta_{21} - \theta_{22})} \tag{14}$$

The terms d_{12} and d_{21} are not physically realizable when $(\theta_{12} - \theta_{11}) < 0$ or $(\theta_{21} - \theta_{22}) < 0$. To mitigate this. the first and second columns of D are multiplied by $e^{(\theta_{12} - \theta_{11})}$ and $e^{(\theta_{12} - \theta_{11})}$, respectively [12]. Then the resulting decoupling matrix becomes:

$$D(s) = \begin{bmatrix} e^{-v(\theta_{22} - \theta_{21})} & -\frac{g_{12}}{g_{11}} e^{-v(\theta_{12} - \theta_{11})} \\ -\frac{g_{21}}{g_{22}} e^{-v(\theta_{21} - \theta_{22})} & e^{-v(\theta_{22} - \theta_{21})} \end{bmatrix} \tag{15}$$

such that:

$$v(\theta) = \begin{cases} 1 & \text{if } \theta \geq 0 \\ 0 & \text{if } \theta < 0 \end{cases}$$

2.4.2. Non-Dimensionally Tuned PID (K_N)

A decoupling matrix is initially employed to mitigate process coupling. Subsequently, a secondary-order model is derived for the obtained process, facilitating the development of a decentralized PI/PID controller through a non-dimensional tuning method. There are three possibilities for the resulting design based on pole-zero positions. Three scenarios are outlined and dedicated decouplers are developed accordingly [13]. These include:

1. When there are no right half poles and right half zeros in the off-diagonal and diagonal elements of D, respectively:

$$D(s) = \begin{bmatrix} w_1(s) & d_{12}(s)w_2(s) \\ d_{21}(s)w_1(s) & w_2(s) \end{bmatrix} \tag{16}$$

Then,

$$w_1(s) = \begin{cases} 1 & if & \theta_{21} \geq \theta_{22} \\ e^{(\theta_{21} - \theta_{22})} & if & \theta_{21} < \theta_{22} \end{cases} \tag{17}$$

$$w_2(s) = \begin{cases} 1 & if & \theta_{12} \geq \theta_{11} \\ e^{(\theta_{12} - \theta_{11})} & if & \theta_{12} < \theta_{11} \end{cases} \tag{18}$$

$$d_{12}(s) = -\frac{g_{12}}{g_{11}} e^{-(\theta_{12} - \theta_{11})}$$

$$d_{21}(s) = -\frac{g_{21}}{g_{22}} e^{-(\theta_{21} - \theta_{22})} \tag{19}$$

This is identical to the lead-lag decoupling system outlined in (15).

2. When there are no right half poles and no right half zeros in the diagonal and off-diagonal elements of $D(s)$, respectively:

$$D(s) = \begin{bmatrix} d_{11}(s)w_3(s) & w_3(s) \\ w_4(s) & d_{22}(s)w_4(s) \end{bmatrix} \tag{20}$$

$$w_3(s) \quad = \quad \begin{cases} 1 & if & \theta_{22} \geq \theta_{21} \\ e^{(\theta_{22} - \theta_{21})} & if & \theta_{22} < \theta_{21} \end{cases} \tag{21}$$

$$w_4(s) \quad = \quad \begin{cases} 1 & if & \theta_{11} \geq \theta_{12} \\ e^{(\theta_{11} - \theta_{12})} & if & \theta_{11} < \theta_{21} \end{cases} \tag{22}$$

$$d_{11}(s) \quad = \quad -\frac{g_{22}}{g_{21}} e^{-(\theta_{22} - \theta_{21})}$$

$$d_{22}(s) \quad = \quad -\frac{g_{11}}{g_{12}} e^{-(\theta_{11} - \theta_{12})} \tag{23}$$

3. When there are right half zeros in the diagonal and off-diagonal elements. This is not addressed in this paper because achieving stability in a decoupler using (19) and (23) is infeasible. Hence, it is beyond the scope of this work. For more details, an interested reader is referred to [13].

2.4.3. Model Predictive Control (MPC)

Model predictive control is a well-known control technique with most recent advancements focusing on its state space representation [37]. MPC computes a sequence of optimized control inputs by optimizing the predicted operations of the plant over a fixed future horizon. Then only the first input is applied to the plant and its output compared to that of the model used for prediction. At each step, the necessary adjustments are made to eradicate any steady-state errors and disturbances. The fundamental idea of MPC is illustrated in Figure 2. Other modelling approaches for predictive control applications are available as documented in [37,38] but we adopt the augmented state space method outlined in [39]. The transformation of the model presented in Equation (2) into a discrete state space representation is feasible. Because of the associated benefits such off-set free control, this work uses the augmented velocity formats as detailed in (24) and (26) [39].
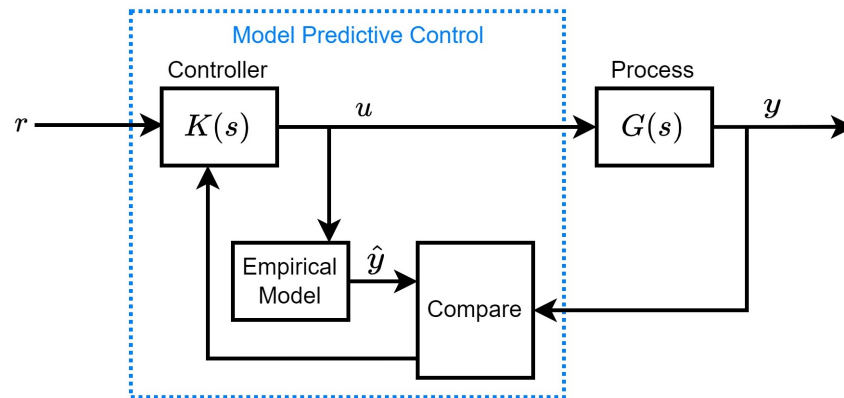
Figure 2. The concept of Model Predictive Control.

$$\begin{aligned} x_p(k+1) \quad &= \quad A_p x_p(k) + B_p u(k) \\ y(k) \quad &= \quad C_p x_p(k) \end{aligned} \tag{24}$$

Then

$$\begin{aligned} x_p(k) \quad &= \quad A_p x_p(k-1) + B_p u(k-1) \\ x_p(k+1) - x_p(k) \quad &= \quad b A_p \big[x_p(k) - x_p(k-1) \big] + B_p [u(k) - u(k-1)] \\ \Delta x_p(k+1) \quad &= \quad A_p \Delta x_p(k) + B_p \Delta u(k) \\ y(k+1) \quad &= \quad C_p x_p(k+1) \\ &= \quad C_p \big[x_p(k) + A \Delta x_p(k) + B_p \Delta u(k) \big] \end{aligned} \tag{25}$$

Consider an extended state $x(k)$ specified as:

$$x(k) = \begin{bmatrix} \Delta x_p(k) \\ y_p(k) \end{bmatrix}, \text{ then } x(k+1) = \begin{bmatrix} \Delta x_p(k+k) \\ y_p(k+1) \end{bmatrix}$$

Then

$$
\begin{aligned}
x(k+1) &= \begin{bmatrix} A_p & 0_n^T \\ C_p A_p & I \end{bmatrix} \begin{bmatrix} \Delta x_p(k) \\ y_p(k) \end{bmatrix} + \begin{bmatrix} B_p \\ C_p B_p \end{bmatrix} \Delta u(k) \\
y(k) &= \begin{bmatrix} 0_{n_p} & I_{n_{out}} \end{bmatrix} \begin{bmatrix} \Delta x_p(k) \\ y_p(k) \end{bmatrix}
\end{aligned}
$$

Finally, the state equations are summarized as:

$$
\begin{aligned}
x(k+1) &= Ax(k) + B\Delta u(k) \\
y(k) &= Cx(k)
\end{aligned}
\tag{26}
$$

The following equations cater for the effects of measured disturbances $d(k)$.

$$
\begin{aligned}
x_p(k+1) &= A_p x_p(k) + B_p u(k) + B_d d(k) \\
y_p(k) &= C_p x_p(k) \\
x(k+1) &= Ax(k) + B\Delta u(k) + B_D \Delta d(k) \\
y(k) &= Cx(k)
\end{aligned}
$$

(27)

(28)

where $B_D = \begin{bmatrix} B_p \\ C_p B_p \end{bmatrix}$. The cost function given in (29) penalizes both the tracking error and the change in manipulated variable.

$$J = \sum_{i=1}^{p} \|r(k+1) - y(k+i)\|_q^2 + \sum_{i=1}^{M} \|\Delta u\|_{r_w}^2 \tag{29}$$

where $\|x\|_P^2 = x^T P x$. Let the variable x_0 represent the initial state of $x(k)$ and the vectors $X, \Delta U$ and Y be defined as follows:

$$X = \begin{bmatrix} x(k+1) \\ x(k+2) \\ \vdots \\ x(k+N_p) \end{bmatrix} \qquad \Delta U = \begin{bmatrix} \Delta u(k) \\ \Delta u(k+1) \\ \vdots \\ \Delta u(k+N_c-1) \end{bmatrix} \qquad Y = \begin{bmatrix} y(k+1) \\ y(k+2) \\ \vdots \\ y(k+N_p) \end{bmatrix} \tag{30}$$

A concise form of these prediction equations is:

$$
\begin{aligned}
X &= F_1 x_0 + \Phi_1 \Delta U + \Phi_{d_1} \Delta D \\
Y &= F x_0 + \Phi \Delta U + \Phi_d \Delta D
\end{aligned}
\tag{31}
$$

where

$$F = \begin{bmatrix} CA \\ CA^2 \\ \vdots \\ CA^P \end{bmatrix} \qquad \Phi = \begin{bmatrix} CB & 0 & \dots & 0 \\ CAB & CB & \dots & 0 \\ \vdots & & & \\ CA^{P-1}B & CA^{P-2}B & \dots & CA^{P-M}B \end{bmatrix}$$

The matrices ΔD and Φ_d are defined similarly to ΔU and Φ by substituting $\Delta u = \Delta d$ and $B = B_d$, respectively. With the proper definition of matrices, a compact form of the cost function in (29) is:

$$J = (S-Y)^T \bar{Q}(S-Y) + \Delta U^T \bar{R} \Delta U \tag{32}$$

Such that $S = r(k) \times \begin{bmatrix} 1 & 1 & \ldots & 1 \end{bmatrix}^T$, $\bar{Q} = diag\{q\} > 0$ and $\bar{R} = diag\{r_w\} \geq 0$. The resulting unconstrained and constrained optimal trajectory of manipulated variables are obtained using (33) and (34), respectively.

$$\Delta U = -\left(\Phi^T \bar{Q} \Phi + \bar{R}\right)^{-1} \Phi^T \bar{Q}(Fx_0 + \Phi_d \Delta D - S) \tag{33}$$

$$\min_{\Delta U} \Delta \quad U^T \quad \left(\Phi^T \bar{Q} \Phi + \bar{R}\right) \Delta U + 2\Delta U^T \Phi^T \bar{Q}(Fx_0 + \Phi_d \Delta D - S) + constant$$
$$: \quad M\Delta U \leq N \tag{34}$$

2.5. Simulation Setup

For the simulations carried out in this work, the system is set up as shown in Figure 3. The blocks and signals are defined as in standard control systems with input and output disturbances d_u and d_y, respectively.
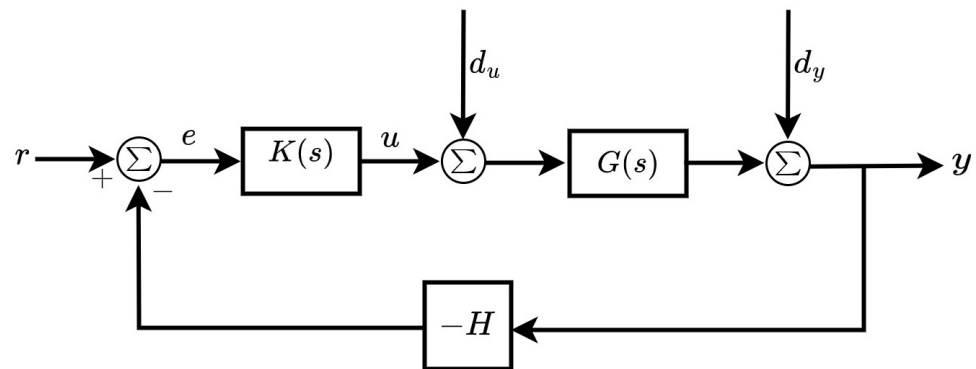
Figure 3. Control problem block diagram.

2.6. Decentralised MPC

Any TITO system such as the process defined by (2) can be subdivided into two interacting subsystems as follows:

$$G_1(s) = \begin{bmatrix} g_{11}(s)e^{-\tau_{11}(s)} & g_{12}(s)e^{-\tau_{12}(s)} \end{bmatrix}$$
$$G_2(s) = \begin{bmatrix} g_{21}(s)e^{-\tau_{21}(s)} & g_{22}(s)e^{-\tau_{22}(s)} \end{bmatrix} \tag{35}$$

The procedure for converting these subsystems into their discrete state space format is straightforward. The resulting configurations of these subsystems, as expressed in Equation (36), solely exhibit interconnections through their inputs; thus, no couplings between the states are present. In this formulation, the inputs to each of the subsystems serves as a measured disturbance in the other subsystem. Any system can be converted to the discrete state space format [20].

$$\begin{aligned} x_{pi}(k+1) &= A_{p_i} x_{p_i}(k) + B p_i u_i(k) + B_{d_i} u_j(k) \\ y_i(k) &= c_{p_i} x_{p_i} \\ i, j &= 1, 2, i \neq j \end{aligned} \tag{36}$$

This can be converted to an augmented model form similar to (26) to give:

$$\begin{aligned} x_i(k+1) &= A_i x_i(k) + B_i \Delta u_i(k) + B_{D_i} \Delta u_{d_j}(k) \\ y_i(k) &= C_i x_i(k) \end{aligned} \tag{37}$$

The resulting prediction matrices for the subsystems are:

$$X_i = F_{1i}x_{i0} + \Phi_{1i}\Delta U_i + \Phi_{d_i}\Delta D_i \tag{38}$$

$$Y_i = F_i x_{i0} + \Phi_i \Delta U_i + \Phi_{D_i}\Delta D_i \tag{39}$$

All the parameters of this equation are defined similarly to the parameters of (31). The predicted measured disturbances for the subsystems are defined according to (40):

$$\Delta D_i = \begin{bmatrix} \Delta u_j(k) \\ \Delta u_j(k+1) \\ \vdots \\ \Delta u_j(k+M-1) \end{bmatrix} \tag{40}$$

Since the inputs for each of the subsystems serve as disturbances to the complementing subsystem, the traditional approach to obtaining the optimal control sequences is to iterate the systems to converge to their Nash equilibrium or Pareto-optima [40]. In this work, we propose a method which avoids iterations but provides good results that are optimal based on model predictions. If the input trajectory calculated at time k is represented by $\hat{D}_i(k)$ according to (41),

$$\Delta\hat{D}_i(k) = \begin{bmatrix} \Delta\hat{u}_j(k) \\ \Delta\hat{u}_j(k+1) \\ \vdots \\ \Delta\hat{u}_j(k+M-1) \end{bmatrix} \tag{41}$$

then the entire sequence is assumed to be optimal at the present time instance which is a valid assumption because of the prediction capability of MPC over the horizon. And to obtain the values of $\Delta\hat{D}_i$ at sample time $k+1$, we use the shifted sequence with the last entry of the sequence repeated to complete the trajectory. The computed input for MPC typically remains constant at the end of the horizon. Therefore, the shifted sequence becomes:

$$\Delta\hat{D}_i(k+1) = \begin{bmatrix} \Delta\hat{u}_j(k+1) \\ \vdots \\ \Delta\hat{u}_j(k+M-2) \\ \Delta\hat{u}_j(k+M-1) \\ \Delta\hat{u}_j(k+M-1) \end{bmatrix} \tag{42}$$

so that there will be no need for iterations and (39) becomes:

$$Y_i = F_i x_{i0} + \Phi_i \Delta U_i + \Phi_{Di}\Delta\hat{D}_i(k) \tag{43}$$

Hence, the problem at hand is to solve two quadratic programming formulations, one for each of the subsystems. These QP problems can be represented in compact form as:

$$\min_{\Delta U_i} \left\{ \Delta U_i^T \left(\Phi_i^T \bar{Q}_i \Phi_i + R_i \right) \Delta U_i + 2\Delta U_i^T \Phi_i^T \bar{Q}_i \left(F_i x_{i0} + \Phi_{Di}\Delta\hat{D}_i - S \right) \right\}$$
$$: \quad M_i \Delta U_i \leq N_i : i = 1, 2 \tag{44}$$

Therefore, there will be a reduction in computational load since the need for iterations has been alleviated. However, the performance of the proposed method may degrade with increasing loop interactions and coupling.

3. Results and Discussion

3.1. Case Study I: Wood and Berry Distilllation Column

Consider the Wood–Berry distillation column model, which is a well-studied 2×2 process model [12,13,41]. The model is given as [29]:

$$
\begin{bmatrix} X_D(s) \\ X_B(s) \end{bmatrix} = \begin{bmatrix} \frac{12.8e^{-s}}{16.7s+1} & \frac{-18.9e^{-3s}}{21s+1} \\ \frac{6.6e^{-7s}}{10.9s+1} & \frac{-19.4e^{-3s}}{14.4s+1} \end{bmatrix} \begin{bmatrix} R(s) \\ S(s) \end{bmatrix} \tag{45}
$$

where $X_D(s)$ is the overhead composition and $X_B(s)$ is the bottom composition, $R(s)$ is the reflux flow and $S(s)$ is the steam flow.

The system was connected according to the simulation setup described in Section 2.5. The performance of the considered controllers was compared in terms of set-point y_{sp} and output disturbance d_y, assuming $d_u = 0$ and $H = 1$.

The RGA is computed as presented (46).

$$
\Lambda = K \otimes H = \begin{bmatrix} 2 & -1 \\ -1 & 2 \end{bmatrix}
$$

The first element $\Lambda_{11} > 1$ implies strong coupling. The decoupling matrices of the PID/PI were obtained using methods discussed in Section 2. The decoupler $D(s)$, given in (46), is the same for the two considered decentralized PID controllers.

$$
D(s) = \begin{bmatrix} 1 & \frac{1.477(16.7s+1)e^{-2s}}{21s+1} \\ \frac{0.34(14.4s+1)e^{-4s}}{10.9s+1} & 1 \end{bmatrix} \tag{46}
$$

The resulting controllers are given as [13]:

$$
K_N = \begin{bmatrix} 0.41 + \frac{0.074}{s} & 0 \\ 0 & -0.12 - \frac{0.024}{s} \end{bmatrix} \tag{47}
$$

$$
K_W = \begin{bmatrix} 0.216 + \frac{0.076}{s} + 0.017s & 0 \\ 0 & -0.068 - \frac{0.019}{s} - 0.064s \end{bmatrix} \tag{48}
$$

Both the MPC and DMPC controllers tuned used a sample time of 1 s, prediction horizon of 20 samples and a control horizon of 4 samples. Similarly, the weightings on the change in MV of 10 and 100 were used for loops 1 and 2 of both controllers, respectively. The controllers were tested for set-point response and output disturbance rejection using step signals with a step size of 0.5. To analyze the input response, step inputs were employed in loops 1 and 2 at 0 and 50 min for the set-point response, respectively. The resulting set-point responses are shown in Figures 4 and 5. Similarly, output step disturbances, also of size 0.5, were applied to loops 1 and 2 at 0 and 50 min, respectively. The plots of the output step disturbance response are shown in Figures 6 and 7.

The plots for both the set-point response and disturbance rejection showed that the predictive controllers had smoother responses without any oscillations and overshoots while the PI/PID controllers had average overshoots of about 20%.

Table 2 presents the mean squared error (MSE) values obtained by the different controllers when comparing their output to the set point. The values of MSE showed that predictive controllers had a similar performance but outperformed the PI/PID controllers, which also had similar performance. A similar trend is observed for the results of the output disturbance rejection presented in the same table.

Overall, the DMPC achieved better results when compared with all the other controllers. The gains achieved by the predictive controllers are expected to be more for constrained processes and processes with larger dead times.
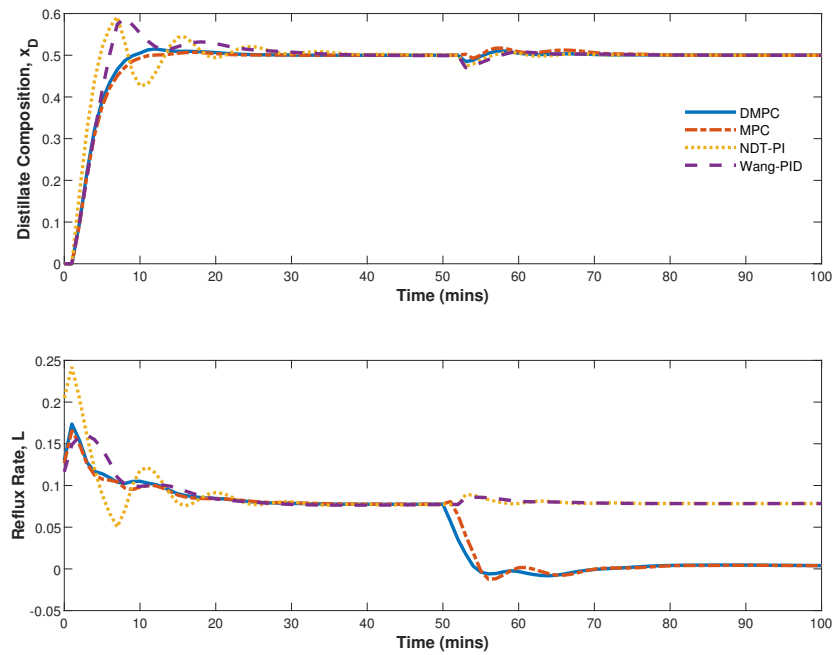
Figure 4. Response of distillate composition of the Wood and Berry distillation column to a step input reference.
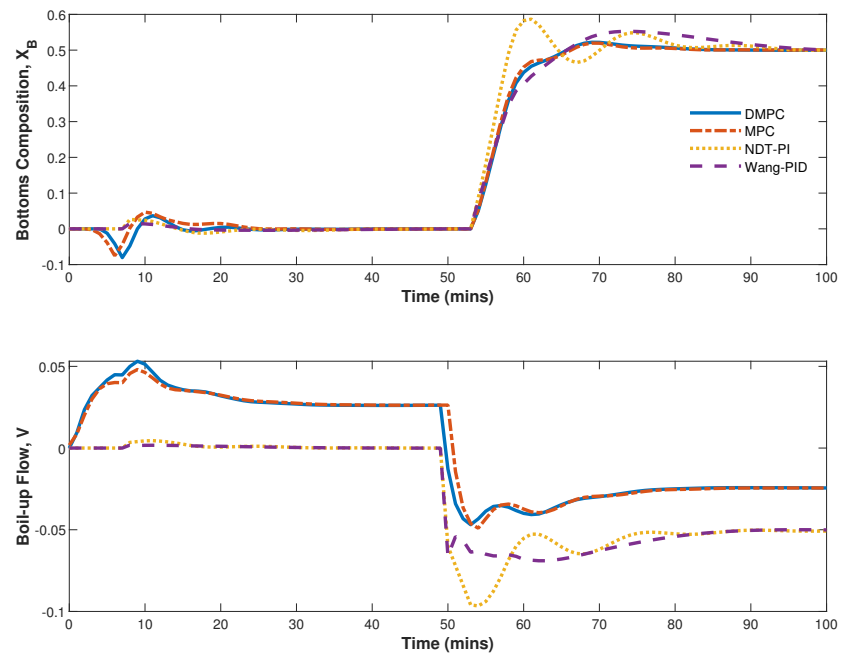

Figure 5. Response of bottoms composition of the Wood and Berry distillation column to a step input reference.
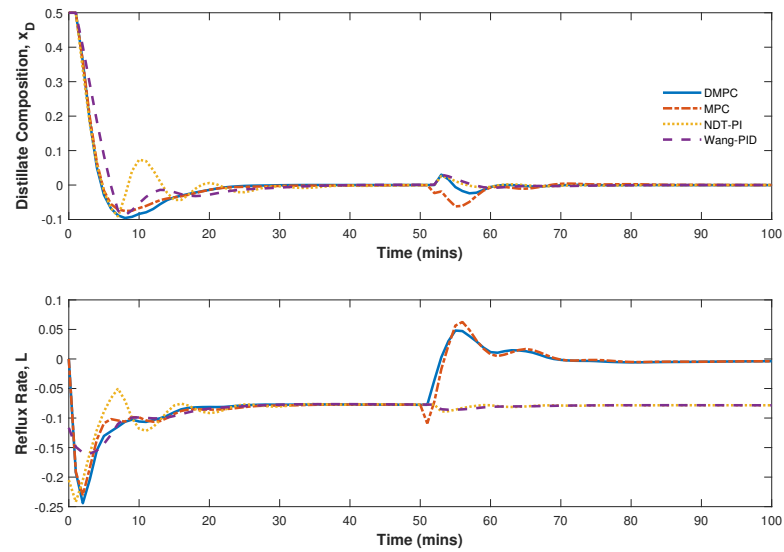
Figure 6. Response of distillate composition of the Wood and Berry distillation column to a step output disturbance.
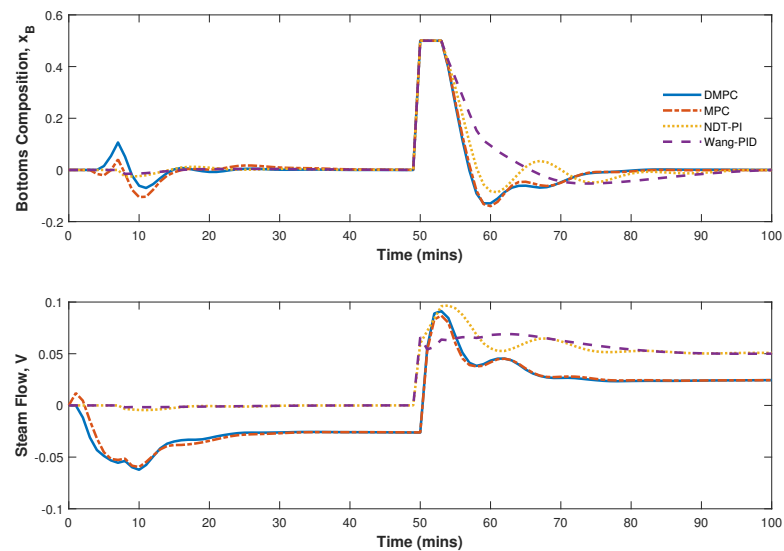

Figure 7. Response of bottoms composition of the Wood and Berry distillation column to a step output disturbance.

Table 2. MSE for all controllers applied to the Wood and Berry distillation column.

Controller	Set-Point Response		Disturbance Rejection	
	X_D	X_B	$X_D \times 10^{-4}$	$X_B \times 10^{-4}$
K_N	0.2438	0.1170	6.7597	1.3616
K_W	0.2454	0.1131	8.1202	1.5143
MPC	0.2414	0.1087	4.7006	1.3415
DMPC	0.2411	0.1088	4.6867	1.3647

It is often not sufficient to evaluate controllers considering output responses alone. Therefore, the total variance (TV) for the controllers was used to study their smoothness based on controller activity, which can imply robustness and greatly affect actuator wear

and tear. The TVs for the controllers were computed using (49). The results presented in Table 3 show that K_W had the least controller activity while K_N had the highest activity. However, for the disturbance rejection case, the PID/PI controller had slightly lower controller activity. In this case, the higher controller activity in the predictive controllers can be justified by their improved performance.

$$TV = \sum_{k=0}^{\infty} \|u(k+1) - u(k)\|. \tag{49}$$

Table 3. TV for all controllers applied to the Wood and Berry distillation column.

Controller	Set-Point Response		Disturbance Rejection	
	X_D	X_B	X_D	X_B
K_N	0.6228	0.1806	0.6228	0.1806
K_W	0.2647	0.1105	0.2647	0.1185
MPC	0.3954	0.1801	0.7079	0.3127
DMPC	0.3824	0.1076	0.6103	0.3041

3.2. Case Study II: High-Purity Distillation Column

The binary distillation column introduced in Section 2 has a steady-state gain matrix of:

$$G = \begin{bmatrix} 0.8754 & -0.8618 \\ 1.0846 & -1.0982 \end{bmatrix} \tag{50}$$

This system has an RGA of 36 and a condition number of 197. Since the magnitudes of the steady-state gains have close values, there is strong interaction between the loops. The large condition number implies that the process is ill conditioned. The step responses of the studied system are shown in Figures 8–11. Careful observation of these responses show both non-linear and directionality of the model.
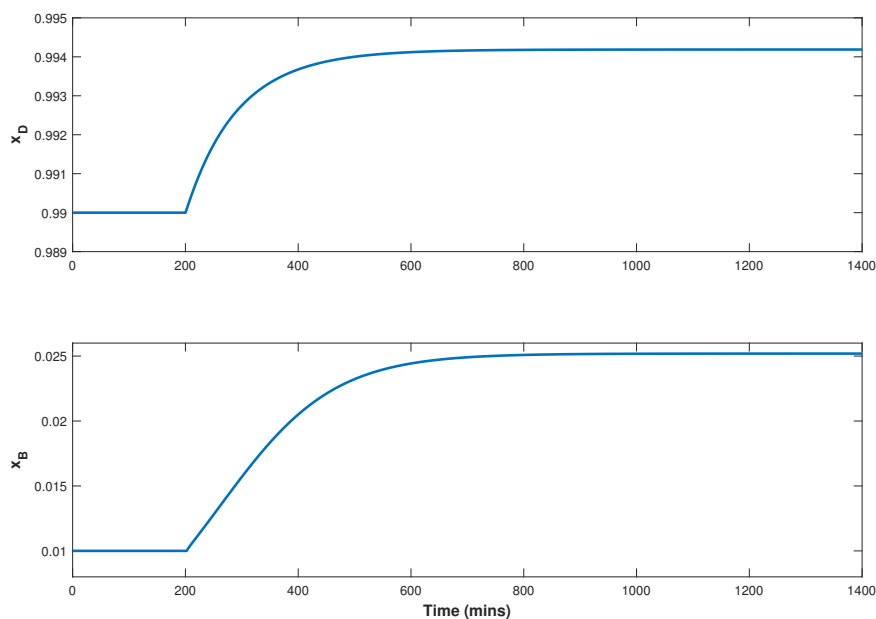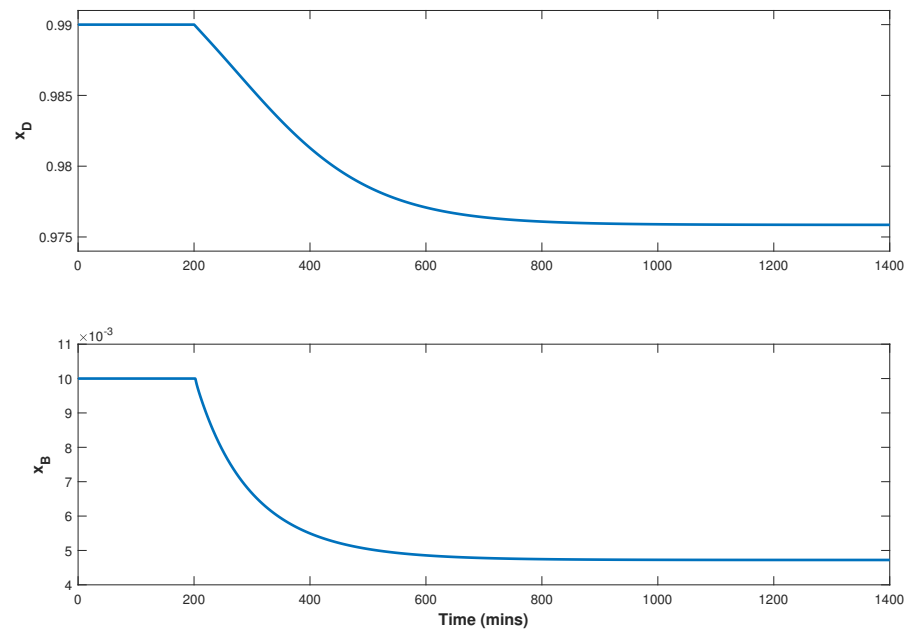

Figure 8. Response to positive step change on *L*.

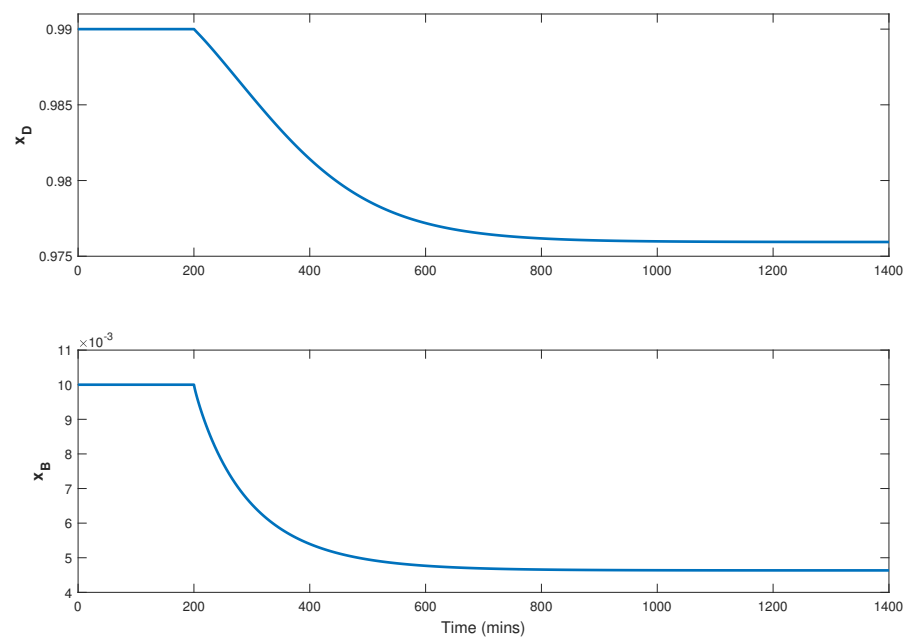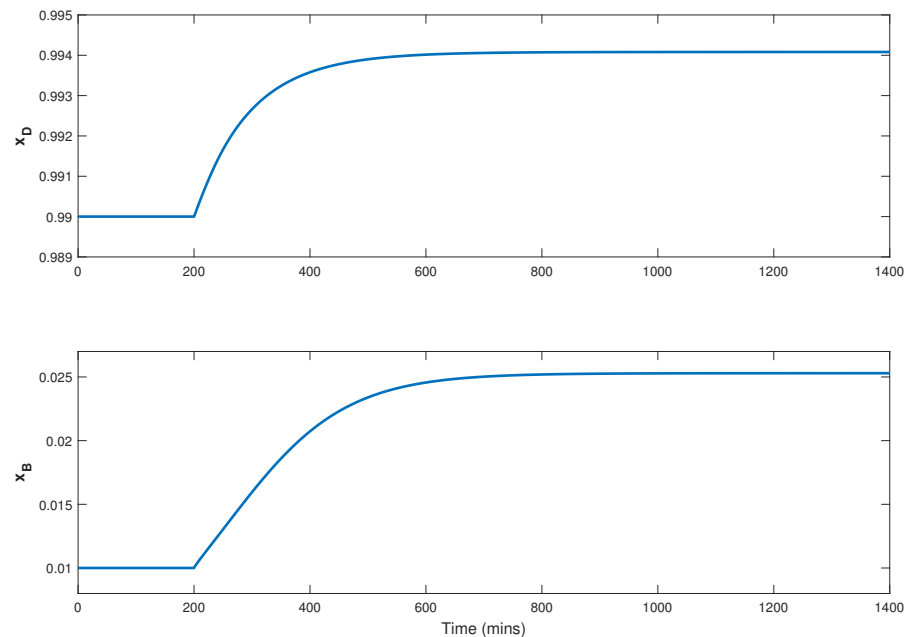**Figure 9.** Response to negative step change on *L*.

Figure 10. Response to positive step change on *V*.

Figure 11. Response to negative step change on *V*.

3.2.1. Identification Tests

The tuning and performance of model-based controllers depends on the quality of the obtained model. Therefore, it is necessary to take steps that would improve system identification. Due to the nature of poorly conditioned processes, unique approaches are required to acquire informative identification data. While normal processes require the use of uncorrelated inputs for system excitation, ill-conditioned processes may require partly correlated signals. Hence, we consider three different sets of identification signals to find the most appropriate for the considered system. These tests were proposed by [4].

1. The use of uncorrelated signals.
    In this method, uncorrelated signals are used to stimulate the plant simultaneously. This is the conventional approach for normal plants. However, studies have suggested that these signals are unlikely to fully excite the process low-gain direction. To address this, two independent pseudo-random binary sequence (PRBS) signals were designed with caution to avoid overexciting the system into strong non-linearity, taking into account the process's non-linearity and directional dynamics. The data collected from this test are displayed in Figure 12. As seen in Figure 13, the process high-gain direction was adequately stimulated while the low-gain direction was hardly excited.

2. The use of partly correlated signals.
    To effectively excite both the high- and low-gain directions in a test signal, a two-period approach is employed. The two periods consist of a low-amplitude uncorrelated period and a high-amplitude identical signal period. During the high-amplitude period, the identical signals excite the low-gain direction, while during the low-amplitude period, the signals move the outputs in opposite directions (effectively moving them in the same direction) to nearly cancel out their effects on the high-gain direction. This approach ensures that both directions are adequately excited. Figure 14 shows the test signal, while Figure 15 shows the resulting output directions. The plot shows that despite using these signals, the low-gain direction was only slightly excited.
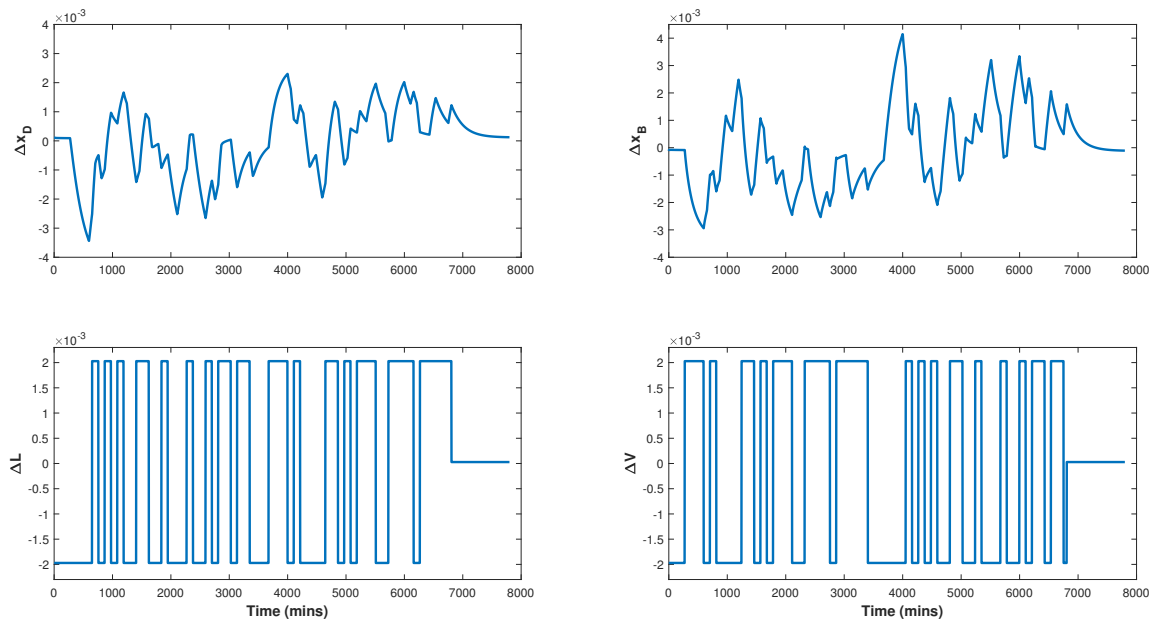
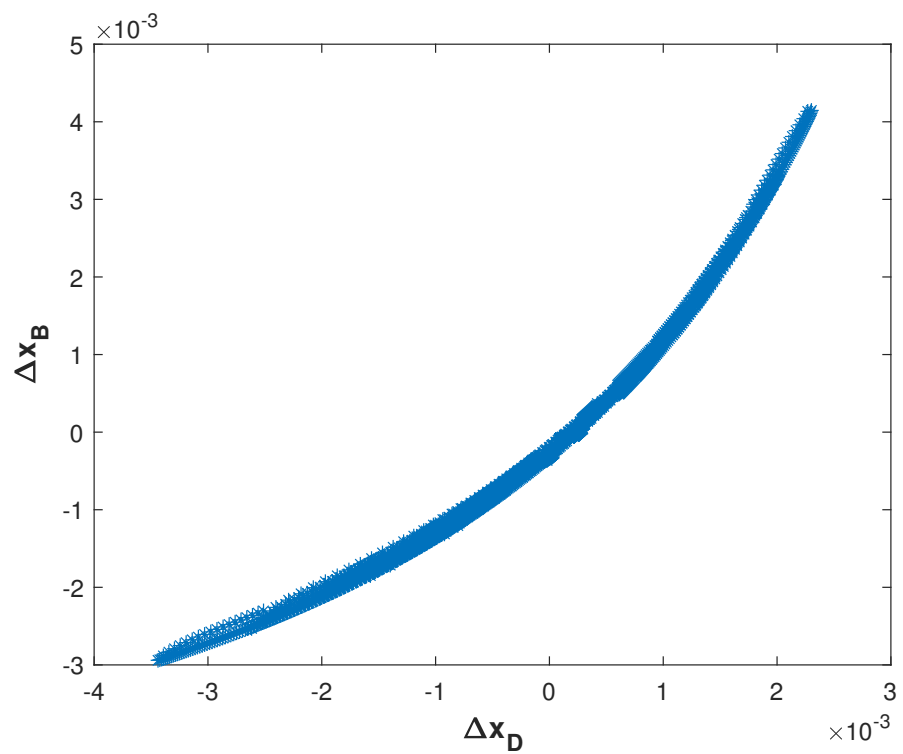**Figure 12.** Plot of plant test data for test with uncorrelated inputs.

Figure 13. Plot of output directions for test with uncorrelated inputs.
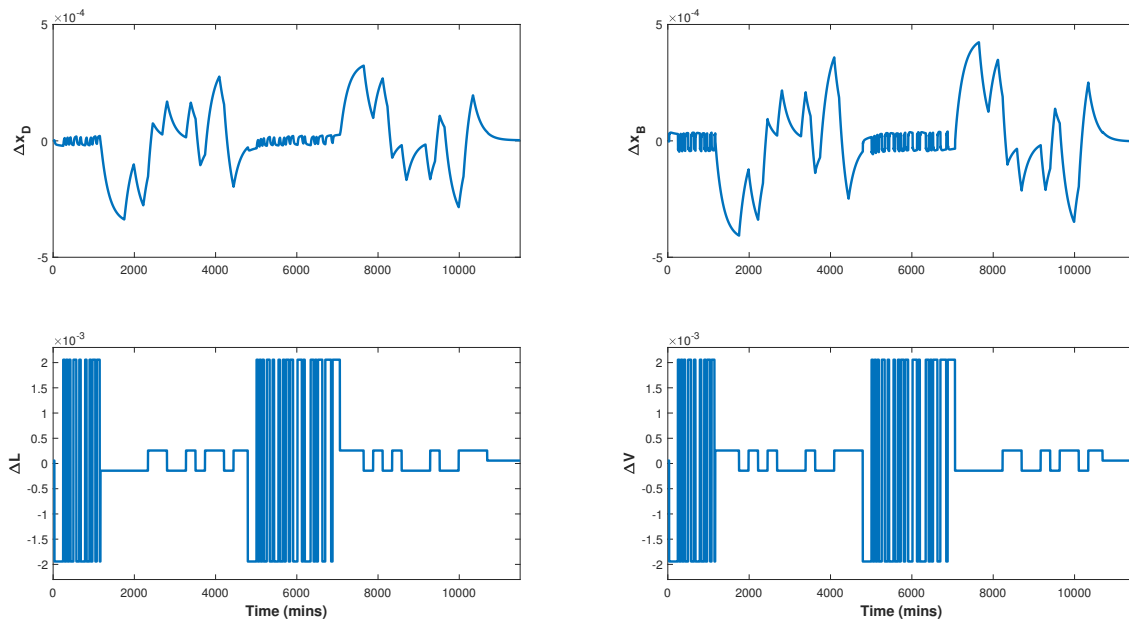
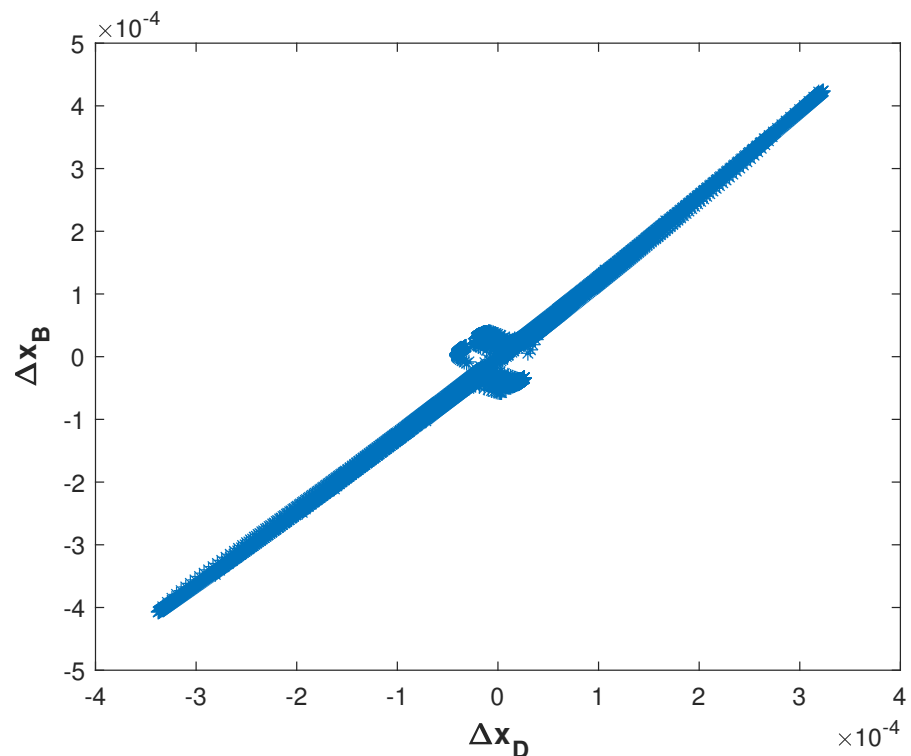**Figure 14.** Plot of plant test data for test with partly correlated inputs.

Figure 15. Plot of output directions for test with partly correlated inputs.

3.　The use of a combination of correlated signals and uncorrelated signals

In this approach, two types of test signals are combined to excite the plant in both high- and low-gain directions. The first type consists of low-amplitude uncorrelated signals, while the second type consists of high-amplitude identical signals. By adding together these two signal types, the high-amplitude signals with the same time intervals can further stimulate the low-gain direction, surpassing the results obtained in previous discussed tests. Meanwhile, the low-amplitude uncorrelated signals excite the high-gain direction. The acquired test dataset and measurements of the plant's output are

depicted in Figure 16, while the output directions are plotted in Figure 17. The figure shows improved excitation of the low-gain direction over the other tests. Hence, the data from this test were used for system identification.
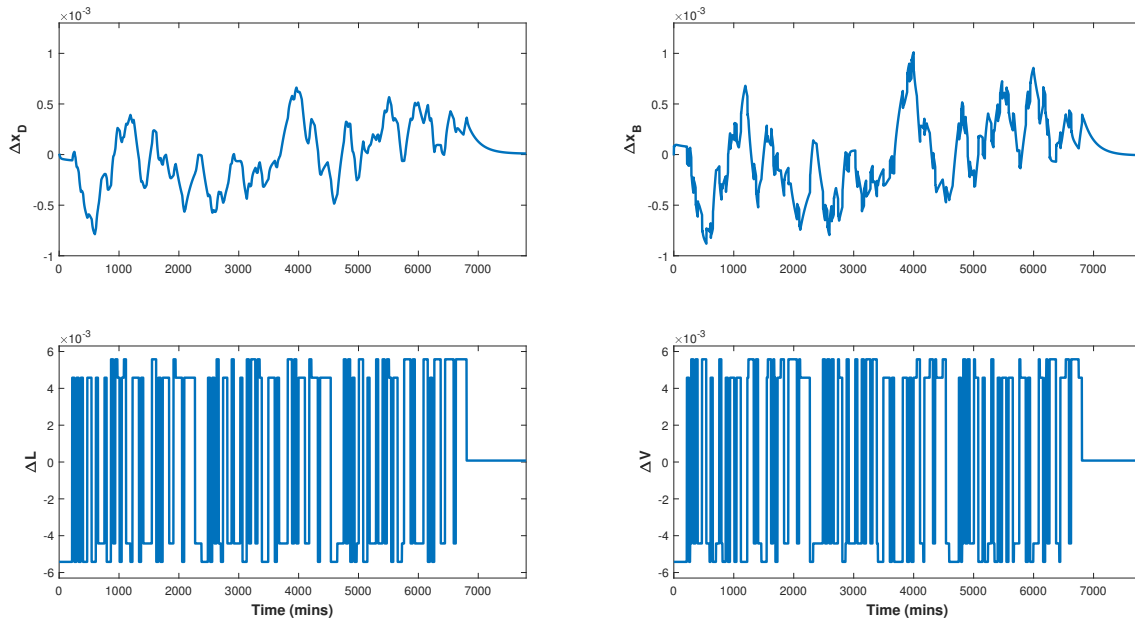

Figure 16. Plot of plant test data for test with sum of correlated and uncorrelated inputs.
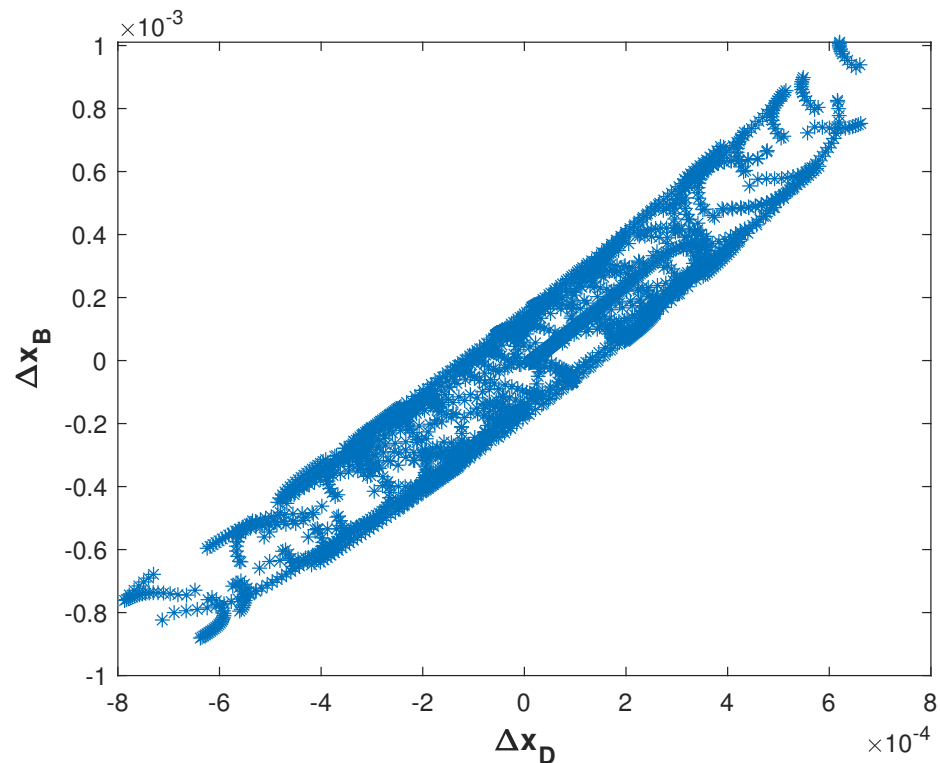

Figure 17. Plot of output directions for test with sum of correlated and uncorrelated inputs.

3.2.2. System Identification

The data collected in the plant tests discussed in Section 3.2.1 were used to identify different models to be considered for controller design. The models obtained from the results of the third test were retained for controller design because, as seen from the tests, this test excites both output directions more than the two other tests. Two different types

of models were developed and compared. A transfer function model is given in (51) and two multi-input single-output (MISO) ARX models are given in (52)–(57).

$$\begin{bmatrix} x_D(s) \\ x_B(s) \end{bmatrix} = \begin{bmatrix} \frac{0.8697}{188.69s+1}e^{-4.278} & \frac{-0.8549}{190.13s+1}e^{-5.325} \\ \frac{1.0739}{189.93s+1}e^{-4.599} & \frac{-1.0876}{188.98s+1}e^{-1.482} \end{bmatrix} \begin{bmatrix} L(s) \\ V(s) \end{bmatrix} \tag{51}$$

The polynomials for x_D are given in (52)–(54) and the corresponding polynomials for x_B are given in (55)–(57). These models gave very good prediction. Hence, they were adopted for controller design.

$$A_1(z) = 1 - 2.418z^{-1} + 2.05z^{-2} - 0.7299z^{-3} + 0.09901z^{-4} \tag{52}$$

$$B_{11}(z) = 0.01238z^{-1} - 0.01672z^{-2} + 0.00653z^{-3} - 0.0007573z^{-4} \tag{53}$$

$$B_{12}(z) = -0.01168z^{-1} + 0.01631z^{-2} - 0.006845z^{-3} + 0.0008076z^{-4} \tag{54}$$

$$A_2(z) = 1 - 1.373z^{-1} + 0.113z^{-2} + 0.2174z^{-3} + 0.04745z^{-4} \tag{55}$$

$$B_{21}(z) = 0.00493z^{-1} + 0.0134z^{-2} - 0.0101z^{-3} - 0.00349z^{-4} \tag{56}$$

$$B_{22}(z) = -0.02159z^{-1} + 0.01073z^{-2} + 0.005933z^{-3} + 0.00009341z^{-4} \tag{57}$$

3.2.3. Control Design

In this case study, we only compare MPC and the proposed DMPC because earlier comparisons with the PID/PI techniques demonstrated improved performance with both MPC and DMPC. Moreover, MPC is considered the benchmark for comparison.

Both the MPC and DMPC controllers were tuned using a sample time of 3 s, prediction horizon of 20 samples and a control horizon of 4 samples. Similarly, for both controllers, the weightings on the change in MV of 0.05 were used for loops 1 and 2. The predictive controllers were tested for set-point response and output disturbance rejection using step signals with a step size of 0.01. To analyze the input response, step inputs were utilized in loops 1 and 2 at 0 and 450 min for the set-point response, respectively. The resulting set-point responses are shown in Figures 18 and 19. Similarly, output step disturbances, also of size 0.01, were applied to loops 1 and 2 at 0 and 450 min, respectively. The plots of the output step disturbance response are shown in Figures 20 and 21.

The MSE obtained for the controllers are shown in Table 4 and the TVs are given in Table 5. From the tables, it is evident that for both set-point tracking and disturbance rejection, DMPC exhibits a slightly lower MAE. DMPC also has higher values of total variance for the set-point response case, signifying more actuator movement. However, the converse is true for the disturbance rejection case. Therefore, the obtained results show that the proposed DMPC gives a performance that is similar to that of traditional MPC and therefore can be considered as a candidate replacement in suitable loops.

Table 4. MSE for predictive controllers applied to the binary distillation column.

| Controller | Set-Point Response | | Disturbance Rejection | |
	$X_D \times 10^{-6}$	$X_B \times 10^{-6}$	$X_D \times 10^{-6}$	$X_B \times 10^{-6}$
MPC	3.869	2.801	4.024	3.421
DMPC	2.988	2.073	3.237	2.687

Table 5. TV for predictive controllers applied to the binary distillation column.

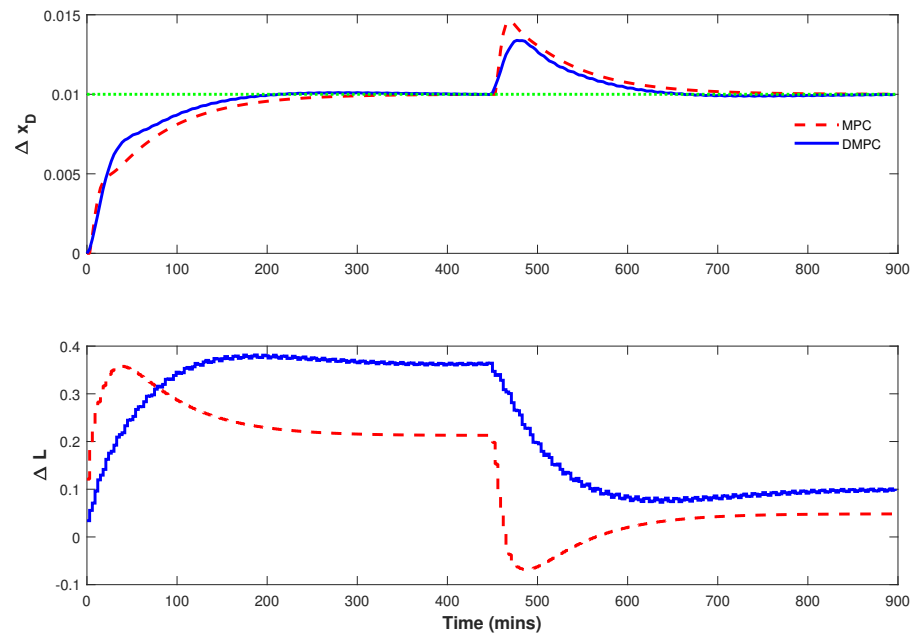| Controller | Set-Point Response | | Disturbance Rejection | |
	X_D	X_B	X_D	X_B
MPC	0.7793	0.8562	2.1272	1.8121
DMPC	1.3491	1.1555	1.4435	1.1987

Figure 18. Step response of the distillate for case study II.
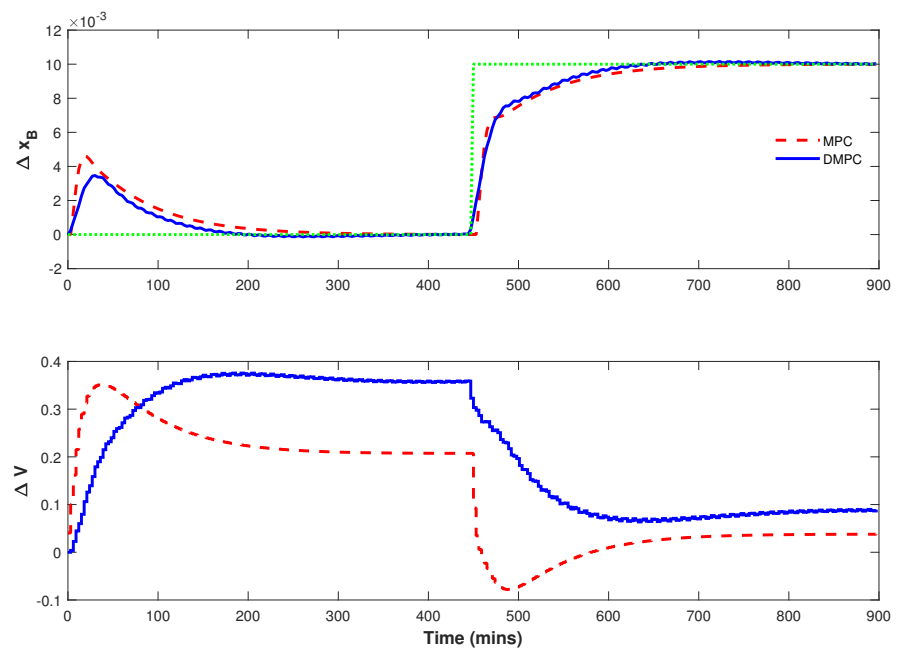

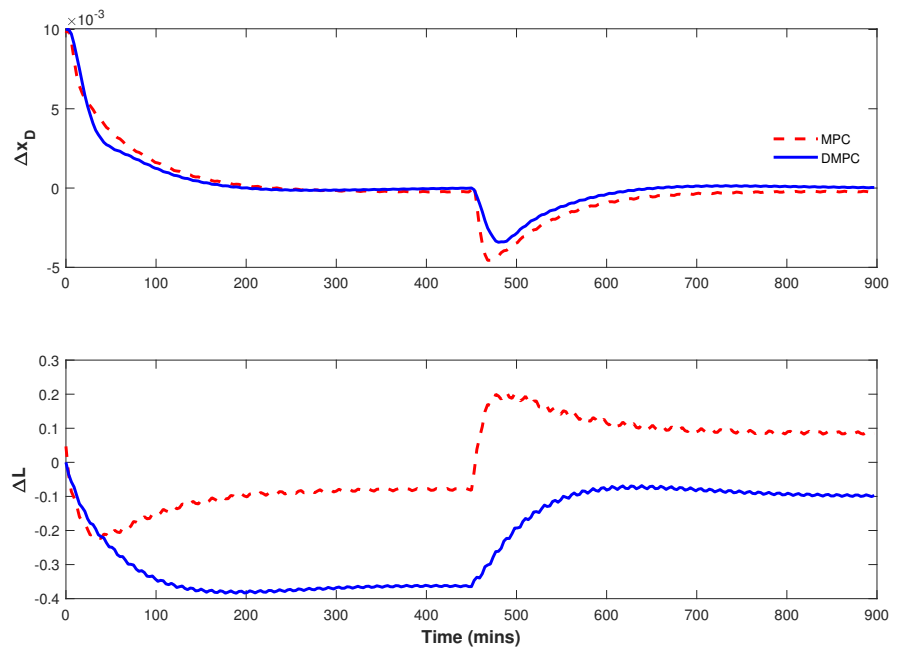**Figure 19.** Step response of the bottoms for case study II.

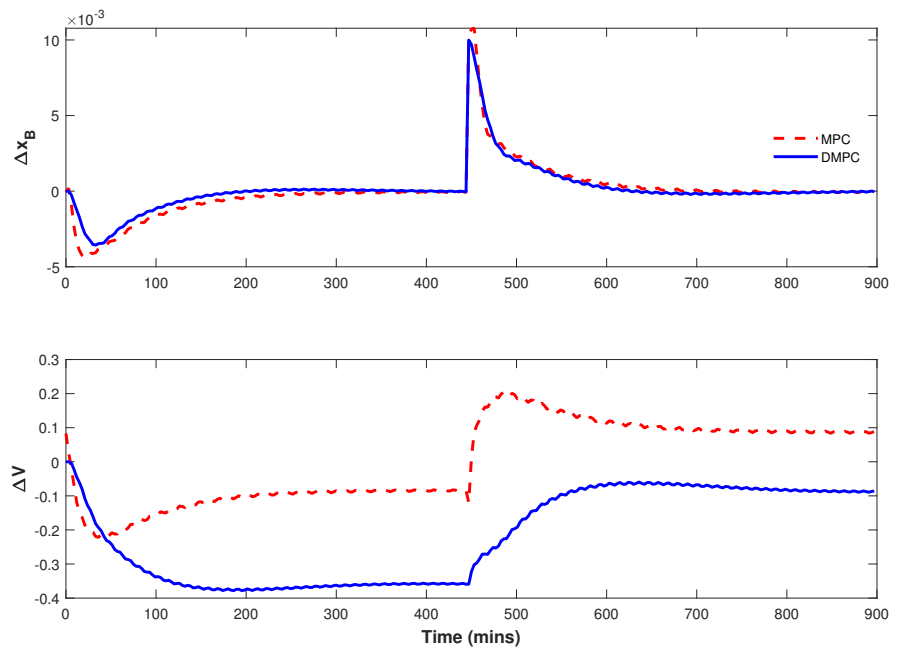**Figure 20.** Step output disturbance response of the distillate for case study II.

Figure 21. Step output disturbance response of the bottoms for case study II.

4. Conclusions

This paper presented the development of a decentralised model predictive control for highly coupled ill-conditioned two-input two-output processes. To achieve this, a detailed process for designing suitable plant tests was presented. The results show that a sum of correlated with uncorrelated signals excited both output directions better. The developed DMPC was also found to outperform well-known decentralised PID controllers while having a comparable performance to the centralised MPC. The technique may also find acceptability amongst practitioners since it allows them to tune the loops in a SISO-like manner. Therefore, the proposed method can be considered as a candidate solution to motivate further adoption of MPC to regulate industrial processes beyond what is currently

obtainable by replacing poorly performing PID loops. The motivation for adopting the proposed technique may be more justifiable in large-scale and networked MIMO systems in which the management of large controllers is a challenge. Therefore, future works will investigate the extension of the proposed method to MIMO systems. This will involve a detailed guidelines on how to incrementally replace existing PID controllers with DMPC on suitable systems. Another area of future work is to study the relative performance of the controllers under constraints.

References

1. Hung, N.T.; Ismail, I.; Saad, N.B.; Tufa, L.; Irfan, M. Design of optimal GBN sequences for identification of MIMO systems. In Proceedings of the 2015 10th Asian Control Conference (ASCC), Kota Kinabalu, Malaysia, 31 May–3 June 2015; pp. 1–6. [CrossRef]
2. Ghosh, R.; Häggblom, K.E.; Böling, J.M. Control-relevant input excitation for system identification of ill-conditioned n × n systems with n > 2. *IFAC Proc. Vol.* **2014**, *47*, 9382–9387. [CrossRef]
3. Yap, T.T.V.; Tan, A.H.; Tan, W.N. Comparison of perturbation signals for ill-conditioned systems and their effectiveness in model-based control. In Proceedings of the 2016 IEEE 12th International Colloquium on Signal Processing & Its Applications (CSPA), Melaka, Malaysia, 4–6 March 2016; pp. 151–156. [CrossRef]
4. Zhu, Y.; Stec, P. Simple control-relevant identification test methods for a class of ill-conditioned processes. *J. Process Control* **2006**, *16*, 1113–1120. [CrossRef]
5. Zhu, Y. *Multivariable System Identification for Process Control [Electronic Resource]*, 1st ed.; Pergamon: Amsterdam, The Netherlands; New York, NY, USA, 2001.
6. Zhu, Y. Multivariable process identification for mpc: The asymptotic method and its applications. *J. Process Control* **1998**, *8*, 101–115. [CrossRef]
7. Darby, M.L.; Nikolaou, M. Identification test design for multivariable model-based control: An industrial perspective. *Control Eng. Pract.* **2014**, *22*, 165–180. [CrossRef]
8. Micchi, A.; Pannocchia, G. Comparison of input signals in subspace identification of multivariable ill-conditioned systems. *J. Process Control* **2008**, *18*, 582–593. [CrossRef]
9. Friman, M. Identification of Ill-Conditioned Systems Using Output Rotation. *IFAC-PapersOnLine* **2020**, *53*, 851–856. [CrossRef]
10. Häggblom, K.E. Easy Ways to Design Inputs to obtain Uncorrelated Outputs in MIMO System Identification. *IFAC-PapersOnLine* **2018**, *51*, 227–232. [CrossRef]
11. Borase, R.P.; Maghade, D.K.; Sondkar, S.Y.; Pawar, S.N. A review of PID control, tuning methods and applications. *Int. J. Dyn. Control* **2021**, *9*, 818–827. [CrossRef]
12. Wang, Q.G.; Huang, B.; Guo, X. Auto-tuning of TITO decoupling controllers from step tests. *ISA Trans.* **2000**, *39*, 407–418. [CrossRef]
13. Tavakoli, S.; Griffin, I.; Fleming, P.J. Tuning of decentralised PI (PID) controllers for TITO processes. *Control Eng. Pract.* **2006**, *14*, 1069–1080. [CrossRef]
14. Lakshmanaprabu, S.; Elhoseny, M.; Shankar, K. Optimal tuning of decentralized fractional order PID controllers for TITO process using equivalent transfer function. *Cogn. Syst. Res.* **2019**, *58*, 292–303. [CrossRef]
15. Aguiar, A.P.V.D.A.; Longhi, L.G.S.; Acioli Júnior, G.; Zani, A.; Barros, P.R. Inverted Decoupling PID Control Applied to the Reactors of a Diesel Hydrotreating Unit. *J. Control. Autom. Electr. Syst.* **2022**, *34*, 315–323. [CrossRef]
16. Ovie, E.; Muazu, M.; Sikiru, T.; Sha'aban, Y. A new hybrid PID-Immersion invariance stabilization control scheme for the RTAC benchmark control system. *Sci. Afr.* **2020**, *8*, e00462. [CrossRef]
17. Bounoua, W.; Aftab, M.F.; Omlin, C.W.P. Controller Performance Monitoring: A Survey of Problems and a Review of Approaches from a Data-Driven Perspective with a Focus on Oscillations Detection and Diagnosis. *Ind. Eng. Chem. Res.* **2022**, *61*, 17735–17765. [CrossRef]
18. Sha'aban, Y.A.; Ikpehai, A.; Adebisi, B.; Rabie, K.M. Bi-Directional Coordination of Plug-In Electric Vehicles with Economic Model Predictive Control. *Energies* **2017**, *10*, 1507. [CrossRef]
19. Kunya, A.B.; Argin, M.; Jibril, Y.; Shaaban, Y.A. Improved model predictive load frequency control of interconnected power system with synchronized automatic generation control loops. *Beni-Suef Univ. J. Basic Appl. Sci.* **2020**, *9*, 47. [CrossRef]
20. Alvarado, I.; Limon, D.; de la PeAa, D.M.; Maestre, J.; Ridao, M.; Scheu, H.; Marquardt, W.; Negenborn, R.; Schutter, B.D.; Valencia, F.; et al. A comparative analysis of distributed MPC techniques applied to the HD-MPC four-tank benchmark. *J. Process Control* **2011**, *21*, 800–815. [CrossRef]

21. Stewart, B.T.; Venkat, A.N.; Rawlings, J.B.; Wright, S.J.; Pannocchia, G. Cooperative distributed model predictive control. *Syst. Control Lett.* **2010**, *59*, 460–469. [CrossRef]

22. Alessio, A.; Barcelli, D.; Bemporad, A. Decentralized model predictive control of dynamically coupled linear systems. *J. Process Control* **2011**, *21*, 705–714. [CrossRef]

23. Sha'aban, Y.; Lennox, B.; Laurí, D. PID versus MPC Performance for SISO Dead-time Dominant Processes. *IFAC Proc. Vol.* **2013**, *46*, 241–246. [CrossRef]

24. Sha'aban, Y.A. The Effect of Dead-Time and Damping Ratio on the Relative Performance of MPC and PID on Second Order Systems. *Appl. Sci.* **2023**, *13*, 1138. [CrossRef]

25. Sha'aban, Y.A.; Tahir, F.; Masding, P.W.; Mack, J.; Lennox, B. Control Improvement Using MPC: A Case Study of pH Control for Brine Dechlorination. *IEEE Access* **2018**, *6*, 13418–13428. [CrossRef]

26. Skogestad, S.; Morari, M. Understanding the dynamic behavior of distillation columns. *Ind. Eng. Chem. Res.* **1988**, *27*, 1848–1862. [CrossRef]

27. Skogestad, S. Dynamics and Control of Distillation Columns: A Tutorial Introduction. *Chem. Eng. Res. Des.* **1997**, *75*, 539–562. [CrossRef]

28. Skogestad, S.; Postlethwaite, I. *Multivariable Feedback Control: Analysis and Design*; John Wiley: Hoboken, NJ, USA, 2005.

29. Seborg, D.E. *Process Dynamics and Control*, 3rd ed.; International Student Version; Wiley: Hoboken, NJ, USA, 2011.

30. Rivera, D.E.; Lee, H.; Mittelmann, H.D.; Braun, M.W. Constrained multisine input signals for plant-friendly identification of chemical process systems. *J. Process Control* **2009**, *19*, 623–635. [CrossRef]

31. Potts, A.S.; Romano, R.A.; Garcia, C. Improving performance and stability of MPC relevant identification methods. *Control Eng. Pract.* **2014**, *22*, 20–33. [CrossRef]

32. Brosilow, C.; Joseph, B. *Techniques of Model-Based Control*; Prentice Hall Professional: Upper Saddle River, NJ, USA, 2002.

33. Rivera, D.; Lee, H.; Mittelmann, H.; Braun, M. High-Purity Distillation. *Control Syst. IEEE* **2007**, *27*, 72–89. [CrossRef]

34. Garrido, J.; Vázquez, F.; Morilla, F. Multivariable PID control by decoupling. *Int. J. Syst. Sci.* **2016**, *47*, 1054–1072. [CrossRef]

35. Liu, L.; Tian, S.; Xue, D.; Zhang, T.; Chen, Y.; Zhang, S. A Review of Industrial MIMO Decoupling Control. *Int. J. Control. Autom. Syst.* **2019**, *17*, 1246–1254. [CrossRef]

36. Pereira, R.D.; Veronesi, M.; Visioli, A.; Normey-Rico, J.E.; Torrico, B.C. Implementation and test of a new autotuning method for PID controllers of TITO processes. *Control Eng. Pract.* **2017**, *58*, 171–185. [CrossRef]

37. Maciejowski, J.M. *Predictive Control: With Constraints*; Pearson Education: Harlow, UK, 2002.

38. Qin, S.; Badgwell, T.A. A survey of industrial model predictive control technology. *Control Eng. Pract.* **2003**, *11*, 733–764. [CrossRef]

39. Wang, L. A Tutorial on Model Predictive Control: Using a Linear Velocity-Form Model. *Dev. Chem. Eng. Miner. Process.* **2004**, *12*, 573–614. [CrossRef]

40. Scattolini, R. Architectures for distributed and hierarchical Model Predictive Control—A review. *J. Process Control* **2009**, *19*, 723–731. [CrossRef]

41. Wood, R.; Berry, M. Terminal composition control of a binary distillation column. *Chem. Eng. Sci.* **1973**, *28*, 1707–1717. [CrossRef]